Supplement of The Cryosphere, 20, 6767–6785, 2026
https://doi.org/10.5194/tc-20-6767-2026-supplement
© Author(s) 2026. CC BY 4.0 License.



The Cryosphere Open Access EGU

Supplement of

Seasonal biases induced by illumination changes and shadow casting in remote sensing derived glacier flow velocities

Laurane Charrier et al.

Correspondence to: Laurane Charrier (laurane.charrier@univ-grenoble-alpes.fr)

The copyright of individual parts of the supplement might differ from the article licence.

S1. GNSS data

Daily GPS phase processing is performed using the GAMIT module of the GAMIT/GLOBK software. The GAMIT module employs the ionosphere-free linear combination of GNSS phase observables and applies a double-difference technique to eliminate phase biases caused by drifts in the satellite and receiver clock oscillators (Bock et al., 1986). The GLOBK (Global Kalman filter) module then performs a network adjustment of the bias-fixed, loosely constrained solution using a Kalman filter estimation algorithm (Herring et al., 2018). Survey sites on the glacier are processed with respect to a network of 13 IGS (International GNSS Service) stations located at distances ranging from 110 km to 1080 km from Argentière Glacier. We define the reference frame using the well-determined IGS stations, with a priori coordinates in the Eurasian-fixed plate EURA14, by estimating a seven-parameter transformation (Altamimi et al., 2017).

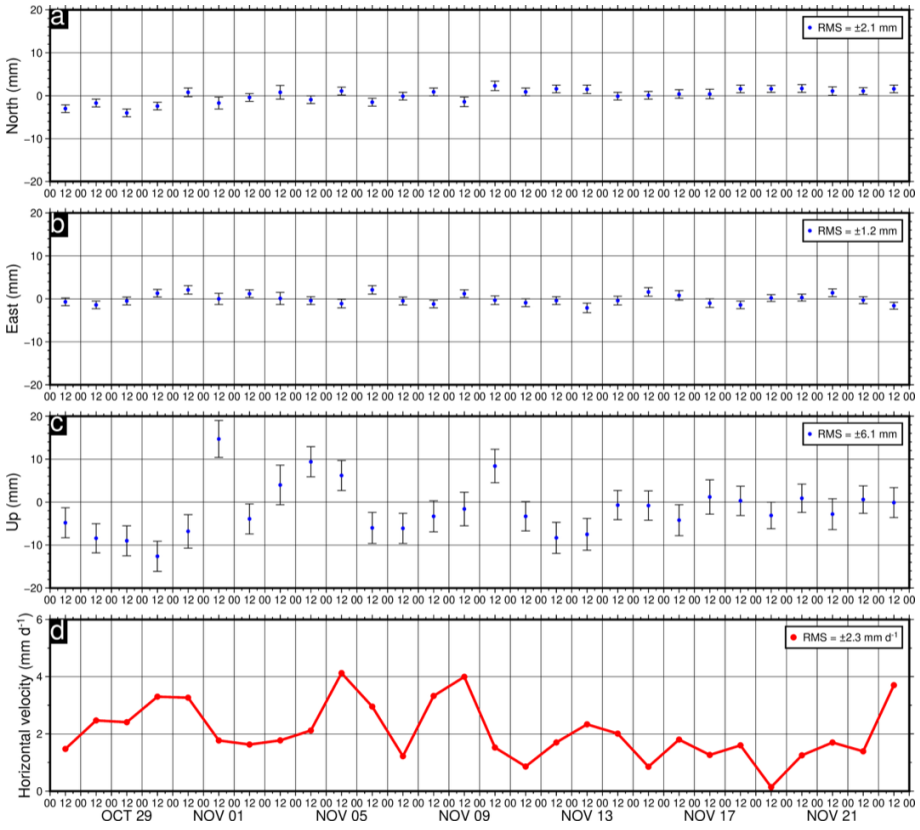


Figure S1. (a-c) Daily position estimates with one standard deviation error bar for the site ARGB in November 2022. (d) Noise level in horizontal velocity determined at the stationary site ARGB for static solutions.

We empirically assess the quality of position estimates using a stationary site ARGB which was intentionally installed on bedrock in November 2022 close to the survey sites on the glacier with a similar multi-path scattering environment. This site serves as a control point because the formal errors generated by the software for a static position estimate are only applicable

to “true” stationary sites. Since Argentière Glacier moves faster than 10 cm per day, GAMIT considers this motion as a formal error in position estimates. Applying these formal errors would violate the least-squares requirement, resulting in overestimated and biased residuals (King, 2004). The position time series of the stationary site ARGB yields an average root-mean-square (RMS) of ±2.1 mm and ±6.1 mm for horizontal and vertical position estimates, respectively (Fig. S1 a–c), and the RMS of "speed" is about 2.3 mm d^{-1} (Fig. S1 d).

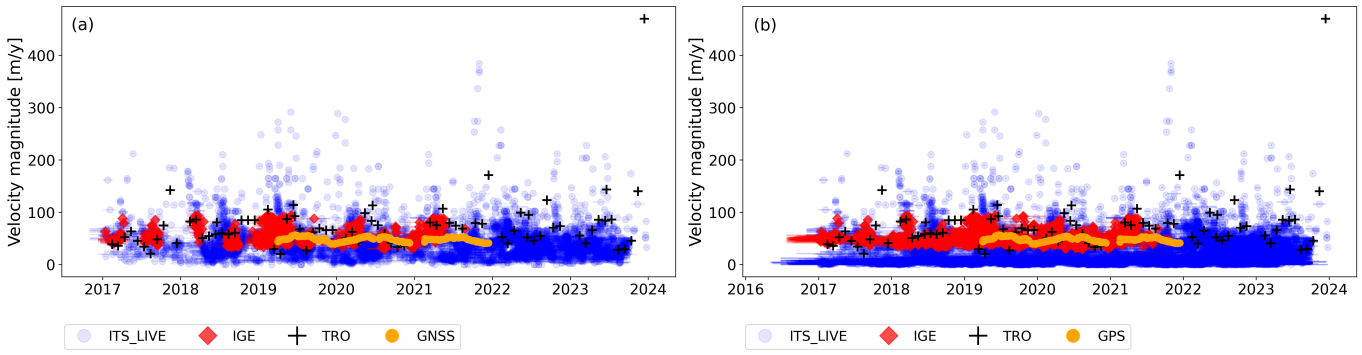


Figure S2. Velocity magnitude at the location of the GNSS antenna installed on the tongue of Argentière Glacier (yellow dots in Fig. 1), measured using a 30-day rolling mean of the GNSS data in orange; and remote sensing datasets "ITS_LIVE with NDC filter" in blue, "IGE with advanced filters" in red and "TRO" in black. (a) Raw velocity estimates from small baseline velocities (< 180 days). (b) Raw velocity estimates from all baseline velocities.

S2. Insight from static areas analysis

S2.1. Active moving areas detected using InSAR

With regard to the InSAR catalog, active moving areas were obtained by visually inspecting 134 Sentinel-1 interferograms (75 and 59 on ascending and descending orbits, respectively) across the entire French Alps. Interferograms were processed using the ForM@Ter LArge-scale multi-Temporal Sentinel-1 InterferoMetry processing chain —FLATSIM— service (Thollard et al.) at different temporal baselines (6, 12, 60 and 360 days).

S3. Origin of seasonal biases

S4. Evidence of seasonal bias in different regions

We compare each of the ITS_LIVE image-pair velocity magnitudes to the GNSS velocity magnitude from (Charrier et al., 2025) on the Lower GNSS station of Kaskawulsh Glacier (Fig. S13). For simplicity, we neglect the temporal baseline and assign each image-pair velocity measurement to the central date of the pair. We stack the difference between the image-pair velocities and the GNSS, i.e., the errors, by day of the year (red dots in Fig. S13). Then, we apply a 30-day rolling median to

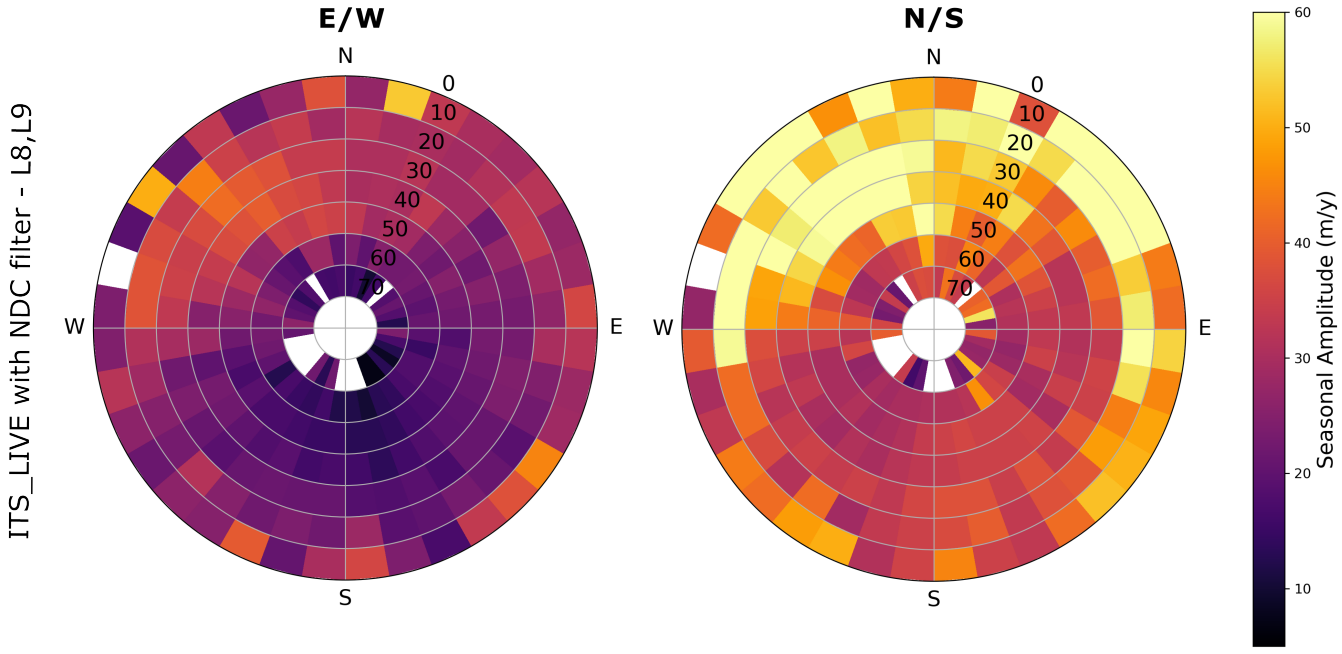


Figure S3. Polar diagram of the median seasonal amplitude of east/west (left) and north/south (right) components of the dataset "ITS_LIVE with NDC filter" using Landsat-8/9 images over static areas. The size of the bin is 10° for both slope and aspect. The slopes are shown along the radial axis, with the highest slopes in the center.

these stacked data (black line in Fig. S13). The errors seem to follow a seasonal pattern with two maxima. This first maximum is reached in spring, around days 120 to 150 of the year while the other is reached in autumn, around days 250 to 300 of the year. This is consistent with the pattern of seasonal bias identified in Section 4.2 and Fig. 5.

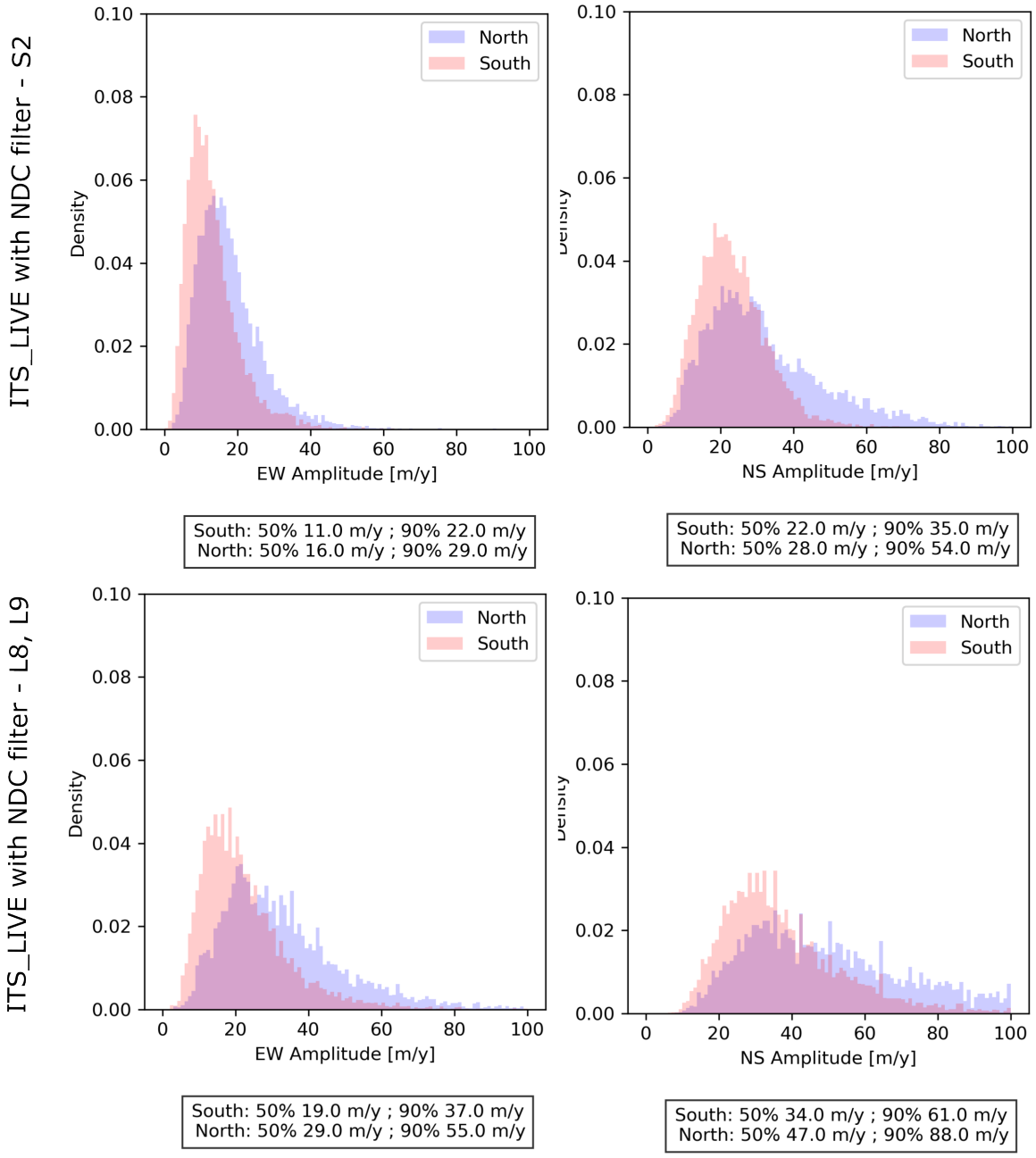


Figure S4. Histograms of the amplitude in static areas of a sinusoidal regression applied to the east/west (left) and north/south (right) components of the datasets "ITS_LIVE with NDC filter" based on Sentinel-2 images (top row) and based on Landsat-8 and 9 images (bottom row). Red bins correspond to south-facing slopes while blue bins represent north-facing slopes. Note the different ranges of the x-axes.

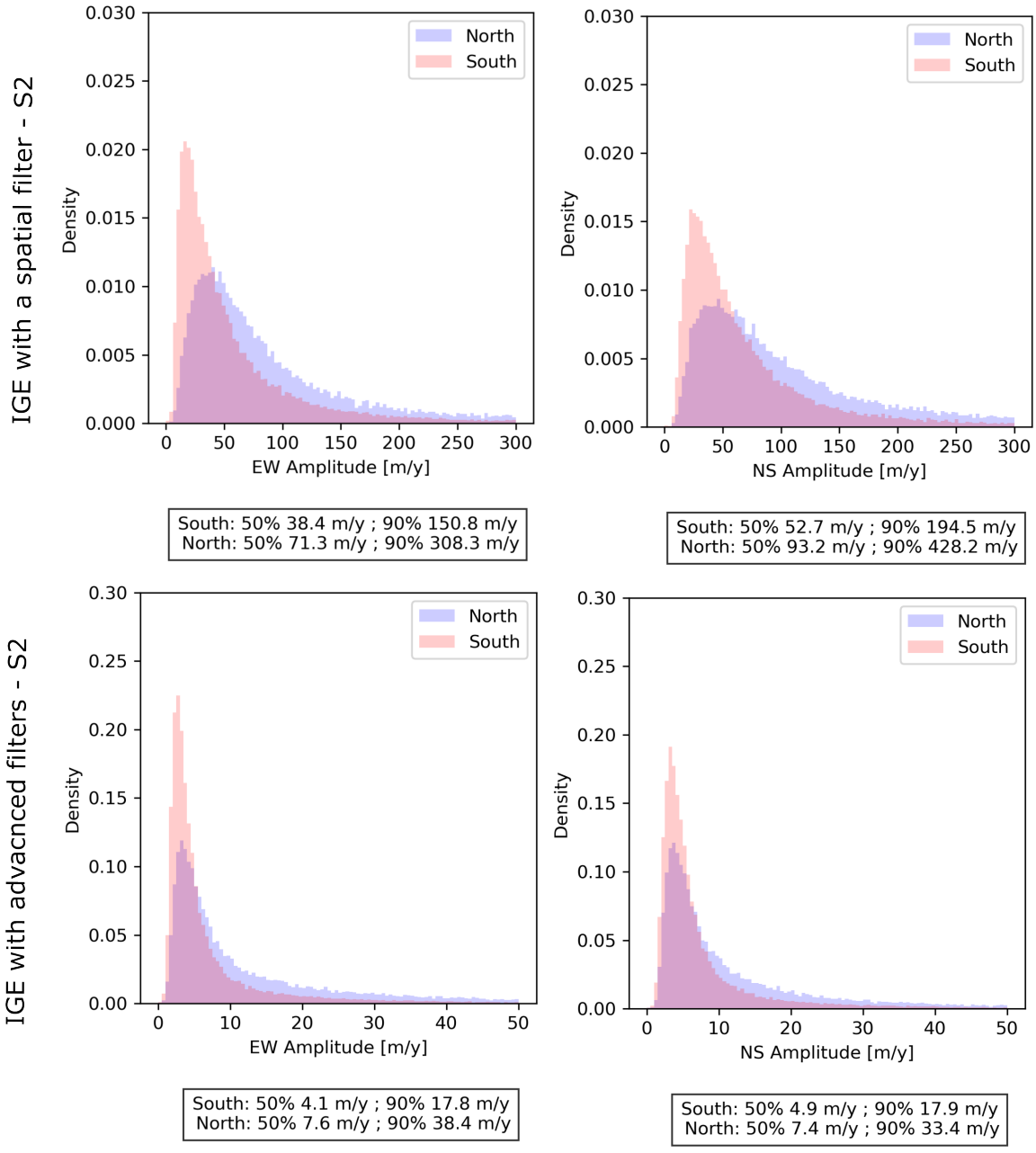


Figure S5. Histograms of the amplitude of a sinusoidal regression applied to the east/west (left) and north/south (right) components of the datasets "IGE with a spatial filter" (top row) and "IGE with advanced filters" (bottom row). Red bins correspond to south-facing slopes while blue bins represent north-facing slopes. Note the different ranges of the x-axes.

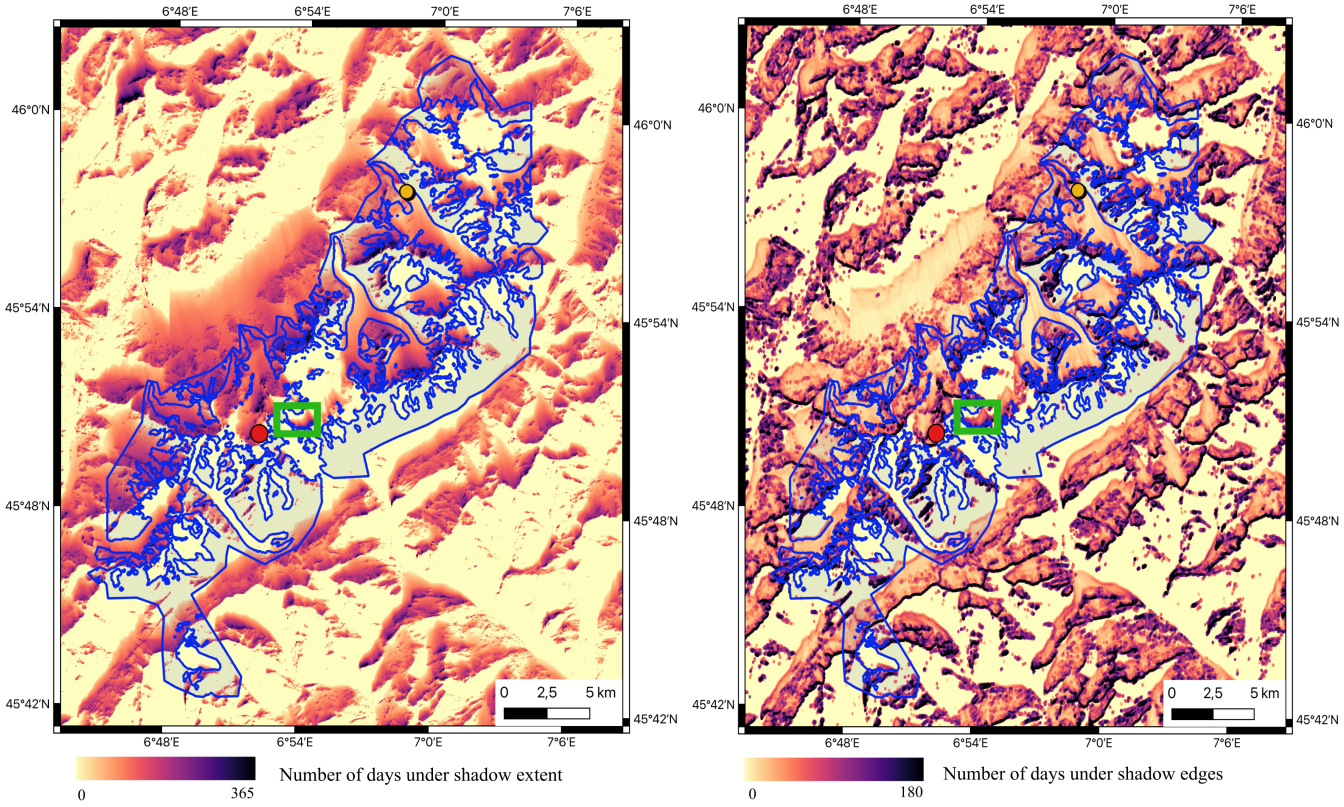


Figure S6. Simulation of the number of days covered by shadow extent (left) and shadow edges (right). The red dot represents the point of coordinate (6.86759°E, 45.83930°N) over the Bossons Glacier given as an example in Fig. 7. The yellow dots correspond to the Arg1 GNSS station. The green rectangle corresponds to Combe Maudite, an area highly affected by shadow casting. The projection of the map is EPSG:32632 and the displayed coordinates are in EPSG:4326.

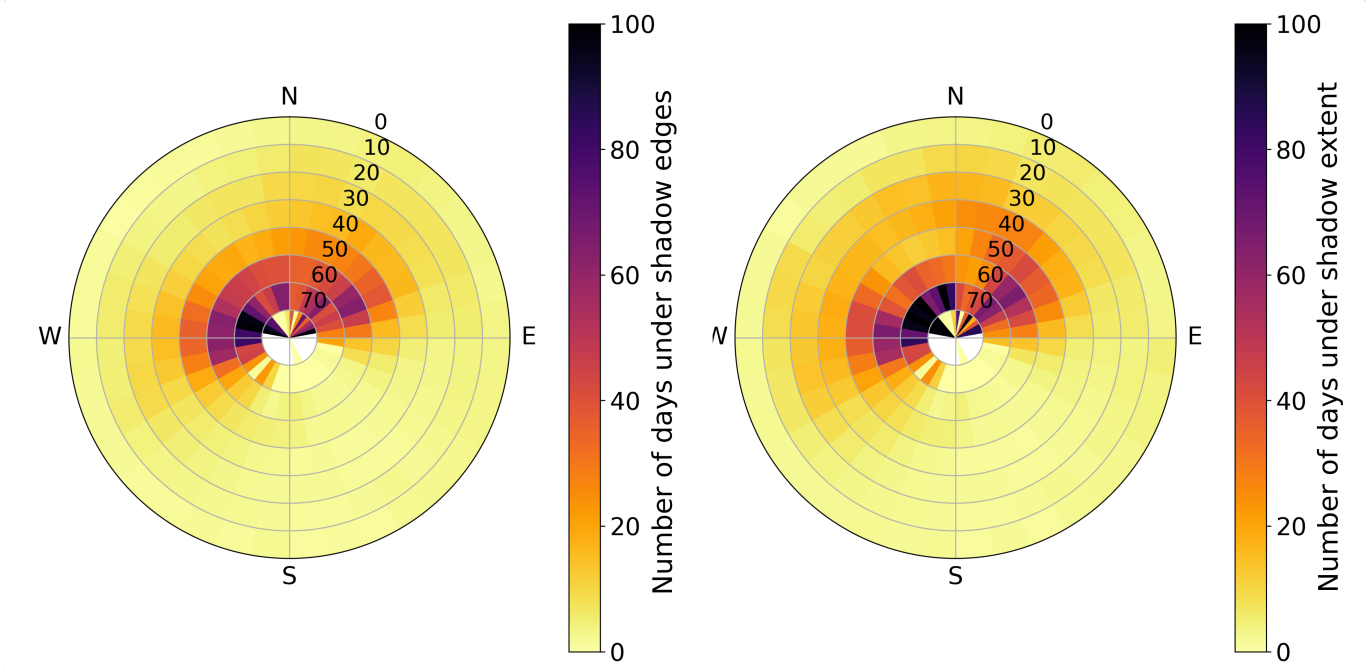


Figure S7. Polar diagram of the number of days under shadow edges (left) and extent (right) over one year for different ranges of aspects and slopes. The simulation has been run over the entire Mont-Blanc Massif.

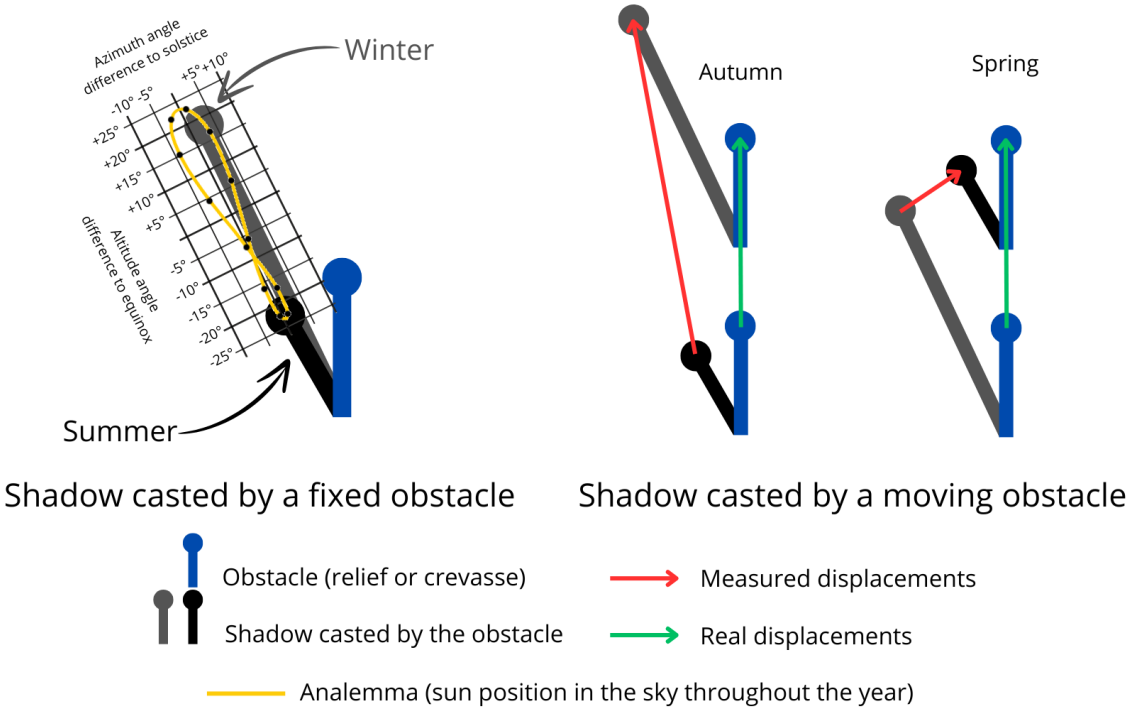


Figure S8. Theoretical illustration of the cast shadow effect. A shadow can be either projected by topography or local relief (crevasses, seracs, etc.), here, moving towards the north. We note that the direction will deviate from the real glacier flow direction depending on the angle between the shadow elongation and the glacier flow direction. The expected movement of a shadow cast through the year is represented by the analemma (in yellow). The shadow cast extends from the winter to the summer solstice and shortens from the summer to the winter solstice. The velocity at which the shadow extends or shortens increases from the summer solstice to the autumn equinox (and from the winter solstice to the spring equinox), and then decreases.

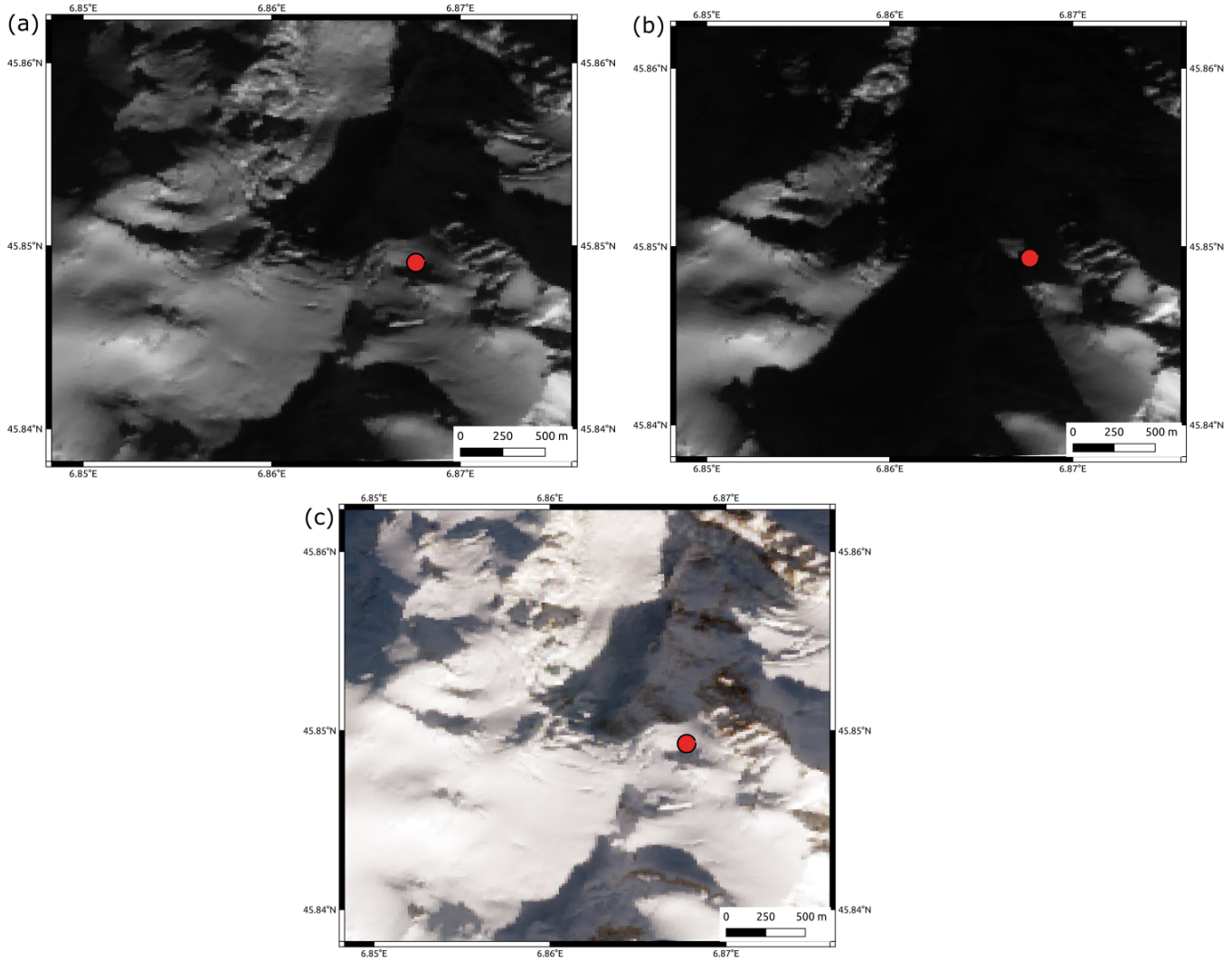


Figure S9. Shadow casting example at the point (6.86759°E, 45.83930°N) over the Bossons Glacier. Sentinel-2 Band 8 images from 10 October 2024 (a) and (b) 04 November 2024. (c) Sentinel-2 True color from 10 October 2024. The location of the area is represented by a yellow rectangle in Fig. S1.

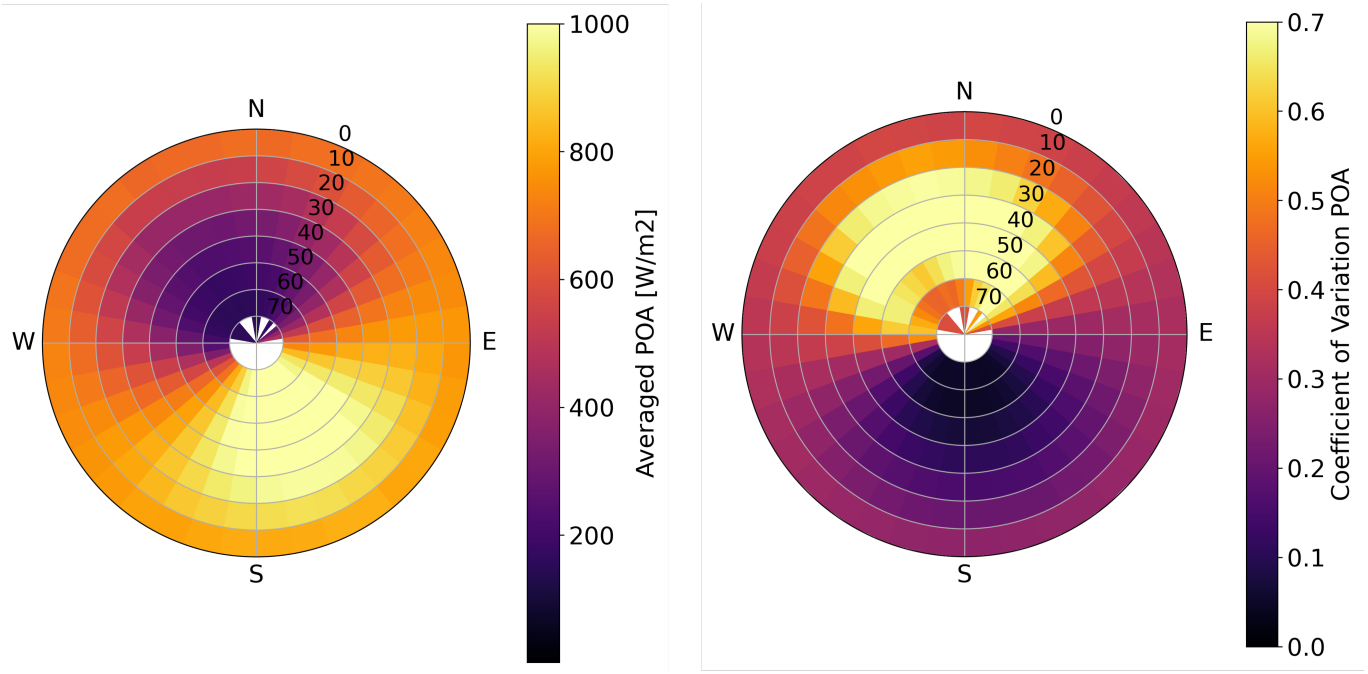


Figure S10. Polar diagram of the average (left) and coefficient of variation (right) of the POA irradiance over the Mont-Blanc Massif for different ranges of aspects and slopes.

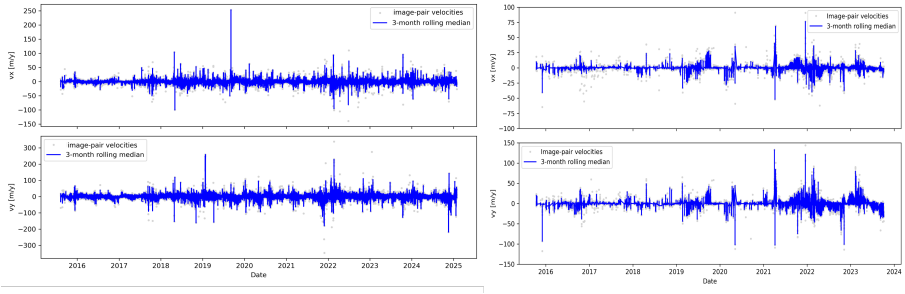


Figure S11. Raw data (light gray) and three-month rolling mean (blue) of velocity over the static areas of the Mont-Blanc Massif for the datasets "ITS_LIVE with NDC filter" (left) and "IGE with a spatial filter" (right). Note the different limits of the y-axis between the left and right figures. Note that we observe no changes in the velocity time series after summer 2021 that could be related to the geometric refinement of the Copernicus DEM used to co-register Sentinel-2 images.

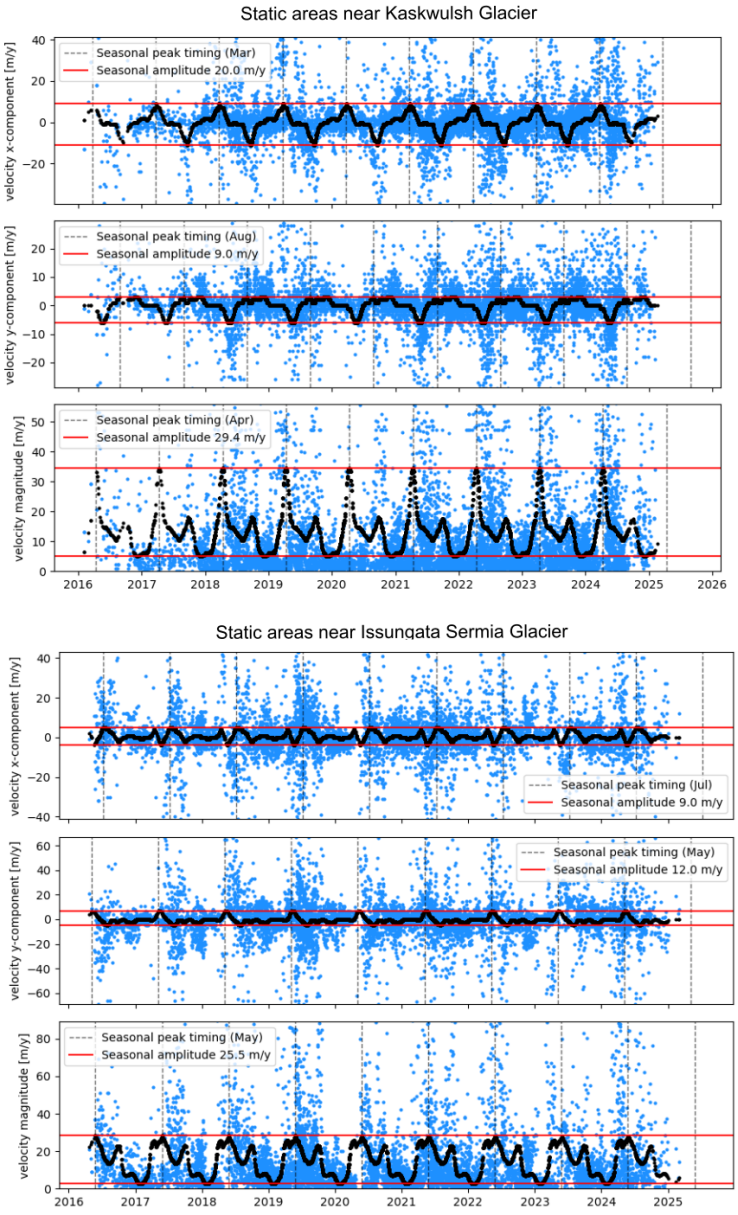


Figure S12. Example of velocity time series over static areas, represented by the two red points in Fig. 10. The coordinates of the points located near Kaskawulsh Glacier and Issungata Sermia are (-138.7238°E, 60.8552°N) and (-50.348547°E,67.339909°N) respectively. Blue dots correspond to ITS_LIVE v2 image-pair velocities. Black dots represent the smoothed velocity time series used to infer seasonal peak timing and amplitude. This time series is computed using a weighted rolling median applied to the image-pair velocities stacked according to their respective day of the year (see Section. 3.2).

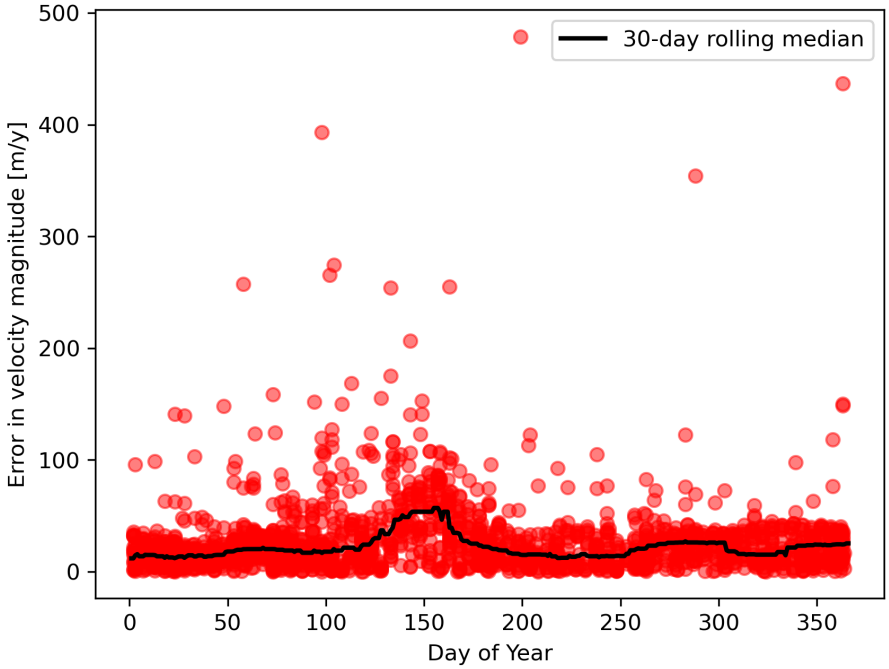


Figure S13. Difference between the velocity magnitude of GNSS and ITS_LIVE image-pair velocities over the the Lower GNSS station of Kaskawulsh Glacier (Charrier et al., 2025).